



EESAP15

INTERNATIONAL CONFERENCE 2024

22-23 OCTOBER

DONOSTIA / SAN SEBASTIÁN

PROCEEDINGS BOOK



eman ta zabal zazu



Universidad
del País Vasco

Euskal Herriko
Unibertsitatea

CIP. Biblioteca Universitaria

Congreso Internacional sobre Eficiencia Energética y Sostenibilidad en Arquitectura y Urbanismo (15º. 2024. San Sebastián)

EESAP15 International Conference 2024, 22-23 October Donostia-San Sebastián [Recurso electrónico]: Proceedings book / [organizado por CAVIAR (Calidad de Vida en Arquitectura, UPV/EHU)]. – Datos. – [Leioa]: Universidad del País Vasco / Euskal Herriko Unibertsitatea, Argitalpen Zerbitzua = Servicio Editorial, [2025]. – 1 recurso en línea : PDF (80 p.)

Modo de acceso: World Wide Web
ISBN. 978-84-9082-982-0.

1. Arquitectura sostenible – Congresos. 2. Urbanismo - Aspecto del medio ambiente. 3. Economía colaborativa. 4. Innovaciones. I. Universidad del País Vasco/Euskal Herriko Unibertsitatea. Escuela Técnica Superior de Arquitectura.

(0.034)620.9:720(063)



**UDA IKASTAROAK
CURSOS DE VERANO
SUMMER COURSES**

UPV/EHU **caviar**
calidad de vida en arquitectura
quality of life in architecture

Study of thermal comfort through the Sky View Factor and the Mean Radiant Temperature in the city of Burgos, Spain

Elena Garrachón-Gómez¹, Ignacio García², Cristina Alonso-Tristán¹, Benoit Beckers³

¹ Solar and Wind Feasibility Technologies Research Group, SWIFT. Electromechanical Engineering Department. Avda. Cantabria s/n. 09006, Burgos, Spain

² Institute of Smart Cities (ISC), Public University of Navarre, Campus Arrosadía, 31006, Pamplona, Spain

³ In Urban Physics Joint Laboratory, E2S UPPA, Université de Pau et des Pays de l'Adour, 64600, Anglet, France

egarrachon@ubu.es

+34 689 11 54 65

Key Words: Mean Radiant Temperature, Sky View Factor, thermal comfort, vegetation

Abstract:

The vegetation in urban environments can regulate air temperature through the evapotranspiration process, modifying air velocity, or blocking direct solar radiation. Residents are subjected to a wide range of thermal variations due to the varied urban configurations that can be found within the city. Thermal comfort is affected by different environmental factors such as air temperature, wind speed, relative humidity, or mean radiant temperature (T_{MRT}). The primary objective of this study is to examine the impact of varying proportions of vegetative elements in urban spaces with distinct Sky View Factor (SVF) values on the fluctuation of Mean Radiant Temperature (T_{MRT}).

The SVF is estimated from hemispherical photographs taken with a commercial digital camera and a FishEye lens, and T_{MRT} is measured with a black globe thermometer. Both parameters are studied at three locations in Burgos (Spain): the esplanade of the Museo de la Evolución Humana (MEH), on the banks of the Arlanzón river and on the Paseo del Espolón. The three selected locations have different SVF values to test its influence on the T_{MRT} estimation. T_{MRT} measurements are taken during a spring day at two times (morning and afternoon). The results demonstrate the fluctuations in thermal comfort across the different urban configurations and at two different times of the day, illustrating the impact of SVF and climatic variables on T_{MRT} . These findings provide insights into the role of urban elements and vegetation in both horizontal and vertical planes within the city, and highlight the value of this information for the design of green infrastructure in urban planning projects.

1. INTRODUCTION

The presence and geometric configuration of urban elements, such as buildings, trees, street layout, materials, and coverings of different surfaces, directly influence the urban microclimate and, consequently, the visual, thermal, and acoustic comfort of its inhabitants (Yan et al., 2022). In recent decades, besides the geometry of urban elements, the increase in urbanized surfaces and the replacement of natural elements with artificial ones have been altering the thermal and energy balance of these areas, modifying their local climate (Oke, 1987). Many parameters allow the study of urban scene configurations depending on the type of analysis to be conducted.

One of the parameters used in urban planning is the Sky View Factor (SVF) (Gong et al., 2018). The SVF describes geometrically the interactions between the plane elements of a scene and the sky. Specifically, it represents the proportion of the total power received by the plane elements from the sky. The obtained value is proportional to the cosines of the angles formed by the beam with the perpendiculars to the two surfaces and inversely proportional to the square of the distance between them (Beckers, 2009). SVF values range between 0 and 1. A value of 0 occurs when the plane surface is obstructed by several elements (buildings or vegetation) and consequently receives no radiation. Conversely, a value of 1 occurs when the measurement surface receives all radiation from

the sky. Depending on the scale of the study, the SVF can be calculated using the photographic method, capturing a 180° angle with a fisheye lens, or obtaining a panoramic view projected in a hemispherical environment. For large-scale studies, simulation models are often used, where the SVF can be calculated from rasterized 3D urban models (Gong et al., 2018).

The SVF is also a potential indicator of outdoor thermal comfort (Yan et al., 2022) due to its ability to describe the geometric relationship of a specific location from the perspective of radiative energy transfer in that environment (Gong et al., 2018). Despite the widespread use of SVF in various urban thermal comfort research studies, it is advisable to complement it with the estimation of other parameters such as the Mean Radiant Temperature (TMRT).

The Mean Radiant Temperature (TMRT) is defined as the uniform temperature of an imaginary enclosure in which the radiant heat transfer of the human body is equal to the radiant heat transfer in the actual non-uniform enclosure. TMRT is commonly used to characterize the radiation perceived by the human body (ASHRAE, 2017). In thermal comfort studies, it is also essential to determine climatic parameters such as air temperature, relative humidity, wind speed, or direct solar radiation (Venhari et al., 2019). One of the most common methods to estimate TMRT is the black globe thermometer method, developed in the 1930s by Bedford & Warner (1930). Since then, it has been widely used due to its simplicity, as it is an indirect way to derive TMRT (Ouyang et al., 2022).

The main objective of this study is to apply the black globe thermometer methodology in various locations in the city of Burgos (Spain) and analyse the influence of variables such as air temperature or wind speed on the determination of TMRT. Additionally, it aims to show how TMRT can be affected by the SVF of each measurement point.

2. MATERIAL AND METHODS

2.1. Study area

Burgos has an area of 107 km² approximately and it is located in the north-eastern part of the Community of Castilla y León, at an elevation of 865 meters above sea level. Its climate is classified as Cfb (Temperate with no dry season and with warm summer) according to the Köppen-Geiger climate classification (Beck et al., 2018). The locations selected for the calculation of the SVF and the TMRT are situated in the city centre, relatively close to each other (Fig. 1). The measurement points have been chosen considering their position relative to the Arlanzón River and the characteristics of the urban vegetation in the area. As shown in Fig. 1, measurement point 1 is located in the esplanade of the Museo de la Evolución Humana (MEH), very close to the river. Measurement point 2 is situated on the bank of the Arlanzón River, in an area with extensive vegetation cover. Measurement point 3, on the Paseo del Espolón, is influenced by its proximity to the river and also has numerous plant species around it.



Fig. 1: : Measurement point locations in the city of Burgos, Spain.

2.2. Medidas ambientales

The T_{MRT} is estimated, according to ISO 7726 standard (2002), by applying Eq.1:

$$T_{MRT} = \left[(t_g + 273.15)^4 + \frac{h_c}{\epsilon_g \times D^{0.4}} \times (t_g - t_a) \right]^{1/4} - 273.15$$

[1],

where:

T_g is the temperature measured by the black globe thermometer ($^{\circ}\text{C}$);

h_c is the convective heat transfer coefficient at the time of measurement ($\text{W/m}^2\text{C}$);

ϵ_g is the emissivity of the black globe, set at 0.957;

D is the black globe diameter, 0.152 m in this case;

T_a is the air temperature ($^{\circ}\text{C}$).

The convective heat transfer coefficient is determined according to ISO 7726 (2002) by Eq.2:

$$h_c = 1.1 \times 10^8 \times V_a^{0.6}$$

[2],

where V_a is the wind speed (m/s).

The black globe thermometer method was originally developed for indoor environments, where the film coefficient is usually very low due to air stagnation and the near absence of forced convection (very low V_a values). In outdoor environments, air typically moves at higher speeds, increasing the

film coefficient more significantly than represented by Eq. 2. For this reason, the black globe thermometer method tends to overestimate the TMRT (Chen et al., 2014). Hence, recalibration based on local climatic conditions is essential. The black globe method performs best when the wind speed is below 0.15 m/s and the air temperature is around 20°C (ISO, 2002).

Other authors have also demonstrated that sampling frequency influences the accuracy of the TMRT estimation method in outdoor environments (Thorsson et al., 2007). In the research conducted by Ouyang et al. (2022), the temporal scale that produced the least dispersion in TMRT data was 5 and 10-minute intervals, similar to the study by Marino et al. (2018), where the most realistic estimates were obtained based on ten-minute intervals.

Air temperature and wind speed were measured manually with the Extech EN510 environmental meter from Teledyne Flir, and black globe temperature was determined with a BLACKGLOBE-L black globe thermometer from Campbell Scientific (Table 1). The measurement frequency was every 10 seconds, averaging the data every 30 seconds. Both devices were installed on two Manfrotto tripods at a height of 1.4 m (Venhari et al., 2019).

Table 1. Technical specifications of the instruments used in the experimental measurements.

| Parámetros | Unidades | Equipo | Empresa | Rango de medida | Precisión |
|----------------------------|----------|---------------|---------------------|-----------------|--------------------|
| Temperatura de globo negro | °C | BlackGlobe-L | Campbell Scientific | -5 a 95°C | ±0.3°C (-3 a 90°C) |
| Temperatura del aire | °C | Extech EN-510 | Teledyne Flir | 0 a 50°C | ±1.2 °C |
| Velocidad del viento | m/s | Extech EN-510 | Teledyne Flir | 0.4 a 20 m/s | ±3% F.S. |

2.3. Experimental measurements and Sky View Factor calculation

The FishEye photographs required to calculate the SVF were taken at the same points where environmental measurements were conducted, using a Canon EOS R5 camera equipped with a CANON EF 8-15 mm F/4L FishEye USM lens. The images were saved in RAW format to maintain the correspondence between the sky radiance captured by the sensor and the signal of the sensor. The basic settings included an ISO of 100, an aperture of f/22, and a focal length of 8 mm. The shutter speed was adjusted based on the specific lighting conditions at each site, with values of 1/160s at MEH, 1/125s at the Arlanzón river bank, and 1/40s at the Paseo del Espolón.

The images were initially projected orthographically and subsequently binarized to compute the point-based SVF using the Nusselt analogy (Beckers et al., 2007). This process involved classifying sky pixels as white and pixels representing other elements, such as vegetation or buildings, as black. The proportion of sky pixels relative to the total pixel count was then calculated using Matlab R2024a software.

3. RESULTS AND DISCUSSION

The experimental measurements were conducted on May 23, 2024. On that day, the climatic and radiative characteristics in Burgos are represented in Fig. 2. It was a quite cloudy spring day, as seen in the radiation graph. The maximum, minimum, and mean values of air temperature and wind speed (Table 2) are from data recorded at the measurement station installed by the SWIFT research group on the roof of the Escuela Politécnica Superior Río Vena (Burgos).

Table 2. Maximum, minimum and mean values of air temperature and wind speed on 23 May 2024.

| Parámetro | Valor máximo | Valor mínimo | Valor medio |
|----------------------|--------------|--------------|-------------|
| Temperatura del aire | 18.83°C | 6.07°C | 11.80°C |
| Velocidad del viento | 3.39 m/s | 0.54 m/s | 1.43 m/s |

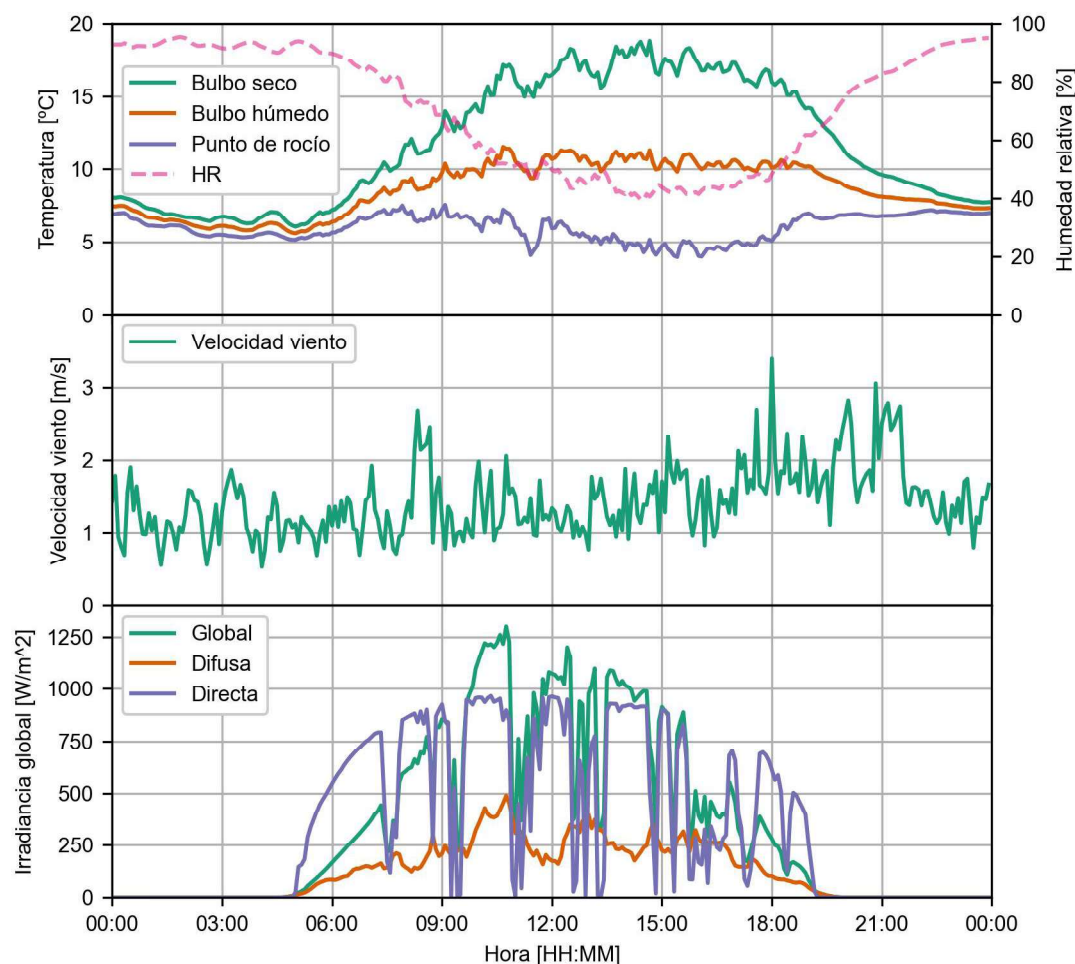


Fig. 2. Climatic and radiative characteristics on 23 May 2024 in the city of Burgos.

The measurement points, represented in Fig. 1, are quite close to each other: there is a distance of about 30 meters between point 1 and point 2, and about 300 meters between point 2 and point 3. The original FishEye photographs can be seen in Fig. 3.



Fig. 3. FishEye images at the three measurements points: a) point 1: MEH, b) point 2: Arlanzón river bank y c) point 3: Paseo del Espolón.

In Fig. 4, the same photographs are shown binarized according to section 2.3. After calculating the percentage of white pixels in each photograph, punctual SVF values were obtained: 0.74 at the MEH, 0.19 on the bank of the Arlanzón River, and 0.57 on the Paseo del Espolón.

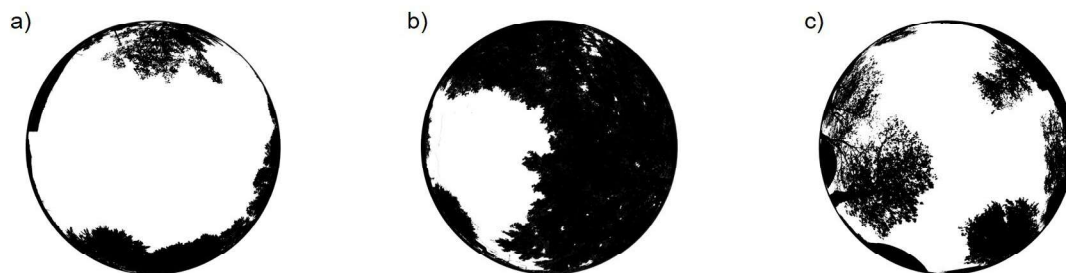


Fig. 4. Binarized images of the three measurements points: a) point 1: MEH, b) point 2: Arlanzón river bank y c) point 3: Paseo del Espolón.

The experimental measurements were conducted at two times on May 23, in the morning and in the afternoon (Figs. 5 and 6). At each point, data collection lasted 10 minutes. As shown in Fig. 5, in the morning, measurements began at the MEH esplanade, then continued at the bank of the Arlanzón River, and finally at the Paseo del Espolón. In both graphs, it is shown that TMRT increases when a wind speed value is recorded. On the other hand, when the wind speed was zero during the 10-minute measurement period (the Paseo del Espolón in the morning and the bank of the Arlanzón River in the afternoon), the TMRT corresponds to the black globe thermometer temperature, independently if the air temperature increases or decreases. It should be noted that the MEH esplanade was in the shade during the morning but in the sun in the afternoon, hence the considerable increase in the black globe thermometer temperature.

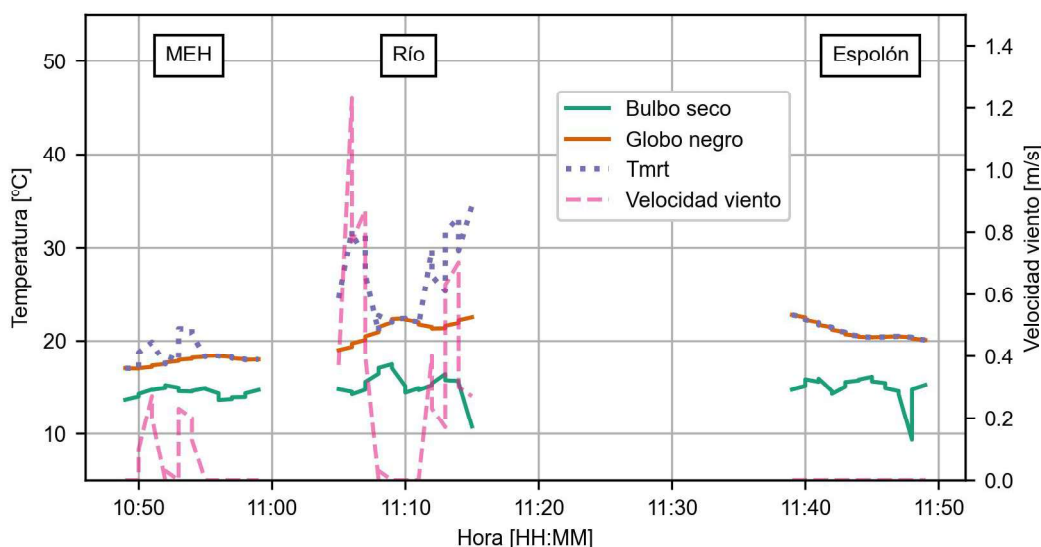


Fig. 5. Measurements of air temperature, black globe thermometer, mean Radiant and wind speed at the three locations during the morning of 23 May 2024.

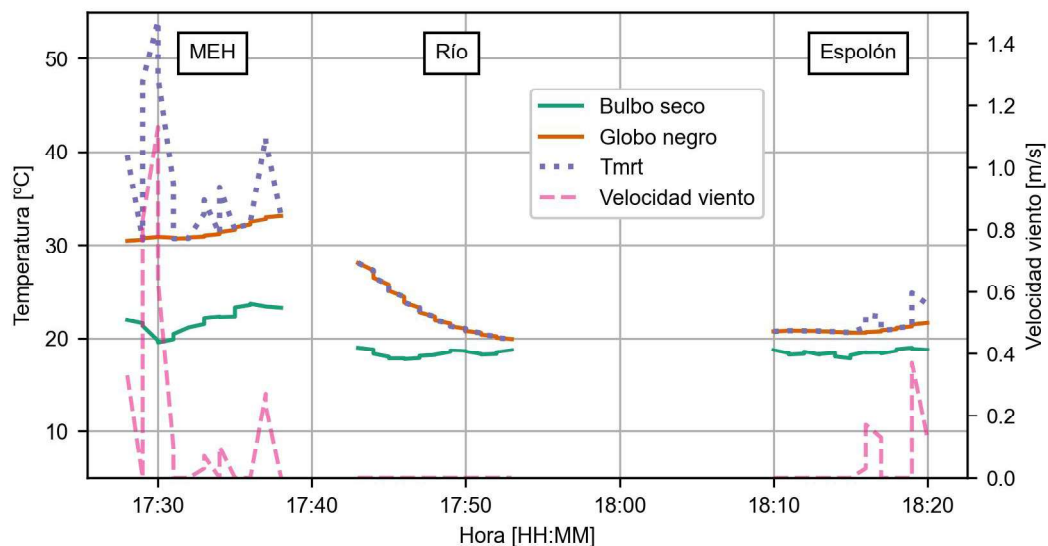


Fig. 6. Measurements of air temperature, black globe thermometer, mean Radiant and wind speed at the three locations during the evening of 23 May 2024.

The observations on the relationship between SVF and urban temperature are somewhat contradictory (Yan et al., 2002). The MEH esplanade has the highest SVF value, but the morning temperatures were lower than on the river bank. In contrast, in the afternoon, temperatures were higher at the MEH than at the river bank, which has a SVF of 0.19. This could be due to other factors, such as ground temperature. On asphalt surfaces with a high SVF value, as the MEH esplanade, the ground temperature is lower early in the morning because it has cooled overnight, and it warms up during the day. Venhari et al. (2019), had also observed lower air temperatures in environments with a lower SVF, due to the presence of buildings and vegetation.

4. CONCLUSIONS

The ISO 7726 standard methodology for calculating TMRT using the black globe thermometer method is very limited for large-scale studies. As demonstrated in this work, environmental conditions are highly variable over time, especially wind speed. This variability makes the estimation of TMRT not sufficiently accurate, and the convective heat transfer factor needs to be adjusted according to local spatial and climatic characteristics. Therefore, a future line of research is proposed to estimate the TMRT of an environment through the processing of photographic images captured in the visible and infrared bands of the electromagnetic spectrum.

Agradecimientos:

This research forms part of project PID2022-139477OB-I00 funded by MCIN/AEI/10.13039/501100011033 and, by “ERDF A way of making Europe”. Elena Garrachón-Gómez expresses her thanks to the Universidad de Burgos for the funding of her pre-doctoral contract.

Bibliografía:

ASHRAE, A. (2017). ASHRAE Standard 55: Thermal environmental conditions for human occupancy. American Society of Heating, Refrigerating and Air-Conditioning Engineers: Atlanta, GA, USA.

Beck, H.E., Zimmermann, N.E., McVicar, T.R., Vergopolan, N., Berg, A., Wood, E.F. (2018). Present and future köppen-geiger climate classification maps at 1-km resolution. *Sci. Data*, 5, 1–12. <https://doi.org/10.1038/sdata.2018.214>

Beckers, B. (2009). Geometrical interpretation of sky light in architecture projects. Proceedings of the international scientific conference on renewables in a changing climate: from nano to urban scale, September 2-3 2009 EPFL, Lau-

sanne, Suisse, Conférence Internationale Scientifique pour le BATiment CISBAT, pp. 231-236. http://www.heliodon.net/downloads/Beckers_2007_Helio_001_en.pdf

Beckers, B., Masset, L., Beckers, P. (2007). Enrichment of the visual experience by a wider choice of projections. Proc. of the 2007 11th International Conference on Computer Supported Cooperative Work in Design, April 26 - 28, 2007, Melbourne, Australia, edited by: Weiming Shen & al, IEEE Catalog Number: 07EX1675C, ISBN: 1-4244-0963-2, Library of Congress: 2007920353.

Bedford, T., Warner, C.G. (1934). The globe thermometer in studies of heating and ventilation, *Epidemiol. Infect.*, 34, 458–473, <https://doi.org/10.1017/s0022172400043242>

Chen, Y.C., Lin, T.P., Matzarakis, A. (2014). Comparison of mean radiant temperature from field experiment and modelling: a case study in Freiburg, Germany. *Theor. Appl. Climatol.*, 118 (3), 535–551. <https://doi.org/10.1007/s00704-013-1081-z>

Gong, F.Y., Zeng, Z.C., Zhang, F., Li, X., Ng, E., Norford, L.K. (2018). Mapping sky, tree, and building view factors of street canyons in a high-density urban environment. *Building and Environment*, 134, 155-167. <https://doi.org/10.1016/j.buildenv.2018.02.042>

Marino, C., Nucara, A., Pietrafesa, M., Polimeni, E., Costanzo, S. (2018). Outdoor mean radiant temperature estimation: is the black-globe thermometer method a feasible course of action? 2018 IEEE International Conference on Environment and Electrical Engineering And 2018 IEEE Industrial and Commercial Power Systems Europe (EEEIC/I CPS Europe), pp. 1–7, <https://doi.org/10.1109/EEEIC.2018.8493714>

Nusselt, W. (1928). Graphische Bestimmung des Winkelverhältnisses bei der Wärmestrahlung. *Z. Ver. Deut. Ing.*, 72 (20), p. 673.

Oke, T.R. (1987). *Boundary Layer Climates*. Routledge.

Ouyang, W., Liu, Z., Lau, K., Shi, Y., Ng, E. (2022). Comparing different recalibrated methods for estimating mean radiant temperature in outdoor environment. *Building and Environment*, 216, 109004. <https://doi.org/10.1016/j.buildenv.2022.109004>

Thorsson, S., Lindberg, F., Eliasson, I., Holmer, B. (2007). Different methods for estimating the mean radiant temperature in an outdoor urban setting. *Int. J. Climatol.*, 27, 1983–1993. <https://doi.org/10.1002/joc.1537>

International Organization for Standardization. (2002). *Ergonomics of the thermal environment. Instruments for measuring physical quantities (UNE 7726: 2002)*.

Venhari, A.A., Tenpierik, M., Taleghani, M. (2019). The role of sky view factor and urban street greenery in human thermal comfort and heat stress in a desert climate. *Journal of Arid Environments*, 166, 68-76. <https://doi.org/10.1016/j.jaridenv.2019.04.009>

Yan, H., Wu, F., Nan, X., Han, Q., Shao, F., Bao, Z. (2022). Influence of view factors on intra-urban air temperature and thermal comfort variability in a temperate city. *Science of the Total Environment*, 841, 1566720. <http://dx.doi.org/10.1016/j.scitotenv.2022.156720>